# Strong bulk photovoltaic effect in chiral crystals in the visible spectrum

Yang Zhang, Fernando de Juan, Adolfo G. Grushin, Claudia Felser, Yan Sun

# Strong bulk photovoltaic effect in chiral crystals in the visible spectrum

Yang Zhang,[1] Fernando de Juan,[2,3] Adolfo G. Grushin,[4] Claudia Felser,[1,5] and Yan Sun[1,*]

[1]*Max Planck Institute for Chemical Physics of Solids, 01187 Dresden, Germany*
[2]*Donostia International Physics Center (DIPC), 20018 San Sebastian, Spain*
[3]*Ikerbasque Foundation, 48013 Bilbao, Spain*
[4]*Institut Néel, 25 Rue des Martyrs, BP 166, 38042 Grenoble Cedex 9, France*
[5]*Center for Nanoscale Systems, Faculty of Arts and Sciences, Harvard University, 11 Oxford Street, LISE 308, Cambridge, Massachusetts 02138, USA*

(Received 23 August 2019; published 19 December 2019)

Structurally chiral materials hosting multifold fermions with large topological number have attracted considerable attention because of their naturally long surface Fermi arcs and bulk quantized circular photogalvanic effect (CPGE). Multifold fermions only appear in metallic states, and therefore most studies so far have only focused on the semimetals in compounds with chiral crystal structures. In this work, we show that the structurally chiral topological trivial insulators are also exotic states, which is interesting from the application point of view, owing to their natural advantage to host a large bulk photovoltaic effect in the visible wavelength region. In recent decades, the shift current in the visible wavelength region was limited to be 10 $\mu A/V^2$ in all the experimentally measured reports. By scanning the insulators with chiral structure, we found a class of compounds with photoconductivity ranging from ~20 to ~80 $\mu A/V^2$, which is comparable to the largest reported shift current. This work illustrates that the compounds with chiral structure can host both quantum CPGE and a strong shift current in the second-order optical response. Moreover, this work offers a good platform for the study of the shift current and its future application by putting the focus on insulators with chiral lattices, so far overlooked in photovoltaic technologies.

DOI: 10.1103/PhysRevB.100.245206

## I. INTRODUCTION

Topological semimetals with multifold fermions protected by chiral crystal structures are becoming a new research frontier in topological materials. Differently from Dirac and Weyl semimetals, the crystal symmetry protects new quasiparticles with large Chern numbers and naturally long surface Fermi arcs [1–6]. Because of the lack of mirror symmetry, a quantized circular photogalvanic effect (CPGE) was theoretically proposed [5,7,8]. The new fermions in chiral crystals have attracted significant attention in the last few years, and the quantized CPGE was experimentally observed very recently [9]. Since multifold fermions only appear in metallic states, considerable attention has been focused on semimetals in this class of compounds, whereas much less attention has been paid to the insulators. Because the chiral crystal structure naturally breaks the inversion symmetry strongly, insulators are ideal candidates for the bulk photovoltaic effect (BPVE) for visible wavelengths. In this work we find strong nonlinear optical response in chiral crystal insulators, which offers another interesting phenomenon from the application point of view.

The utilization of solar energy has been considered as one of the most convincing strategies for future sustainable energy. To date, converting light to electricity via a p-n junction based solar cell is the most powerful technology for solar energy storage. The output of the solar cell is constrained by the detailed balance limit: the probability of photoexciting an electron to a conduction band is balanced by its decay back to a valence band [10]. Hence, searching for new mechanisms to convert the light to electricity is an important and necessary topic. Steady BPVE based on second-order optical response is one of the most promising candidates, where the intrinsic photocurrent is generated by the polarized light in noncentrosymmetric materials [11–22]. The power conversion rate scales quadratically with the BPVE conductivity. Further, the BPVE is determined by the intrinsic electronic band structure of a single crystal, and a photovoltage above the band gap can be achieved via BPVE [19,23]; this is a potential way to overcome the extrinsic limitations for solar power conversion.

Limited by the mechanism of the second-order response, the size of the BPVE generated current is generally much smaller than that from conventional p-n junction photovoltaics [24–26]. In the typical ferroelectric materials of $BaFeO_3$ [24,25], $BaTiO_3$ [27,28], $PbTiO_3$ [24], heterocyclic polymer [29], etc., the shift currents are limited below 10 $\mu A/V^2$ in the visible spectrum. Recently, two theoretical predictions with effective three-dimensional shift current of approximately 100 $\mu A/V^2$ were reported, one with the design strategy of tuning the tight binding (TB) model parameters, and the other with the real compounds of $LiAsS_2$, $LiAsSe_2$, $NaAsSe_2$, and graphitic $BC_2N$ [26,29–33]. However, a real measurement is still absent, which might be due to difficulty in the integration of compounds in experiments. Therefore, real materials with large shift current are desired for both fundamental study and potential applications.

*ysun@cpfs.mpg.de

 

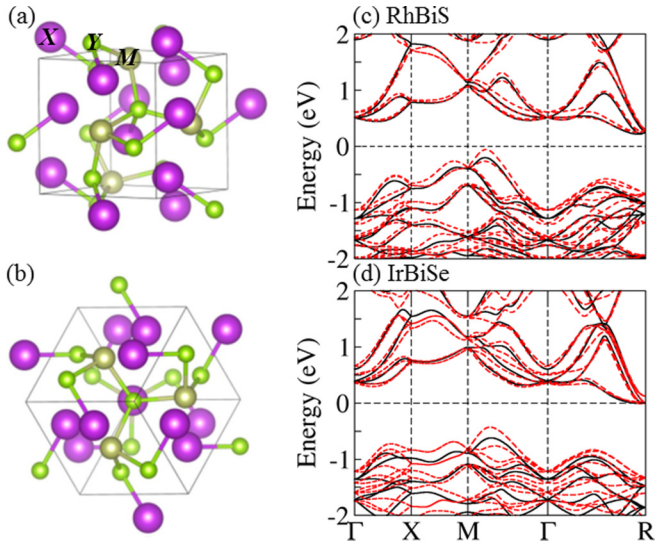


FIG. 1. Representative crystal lattice and electronic band structures for the class of chiral materials discussed in the main text. (a,b) Crystal structure of this class of compounds $MXY$ ($M$ = Ni, Pd, Pt, Rh, and Ir; $X$ = P, As, Sb, and Bi; $Y$ = S, Se, and Te) viewed from different directions. (c,d) Energy dispersions along high symmetry lines for RhBiS and IrBiSe, respectively. The bands without and with the inclusion of spin orbital coupling (SOC) are represented by a solid black line and dashed red line, respectively.

In this work, we have found a group of insulators with chiral lattices where the photoconductivity ranges from ∼20 to ∼80 $\mu A/V^2$, comparable to the largest reported photoconductivity in the insulators and semiconductors. This class of materials is defined by a chiral lattice structure that cannot be obtained by a small interpolation between centrosymmetric and noncentrosymmetric structures. Since the lattice constant is close to the widely used semiconductor CdTe, it should be easy to integrate them into heterostructures for further the study of photovoltaic technologies.

## II. CRYSTAL STRUCTURE AND METHOD

This group of compounds were first synthesized by Hulliger in 1963, with a cobaltite structure belonging to space group $P213$ (No. 198), with a cubic setting, as presented in Figs. 1(a) and 1(b) [34]. By substituting the three atoms in CoAsS by different elements, a class of new compounds $MXY$ (with $M$ = Ni, Pd, Pt, Rh, and Ir; $X$ = P, As, Sb, and Bi; $Y$ = S, Se, and Te) with the same crystal symmetry were synthesized. With the absence of an inversion center, they allow for a nonzero shift current. By considering the different electron fillings, one can further classify them into two subgroups of insulators ($M$ = Rh and Ir) and metals ($M$ = Ni, Pd, and Pt).

The crystal structure in Figs. 1(a) and 1(b) shows that only the transition metal ($M$) sites can be tuned to inversion positions by a small shift (∼3.5% of lattice constants). For the sites $X$ and $Y$, all the atoms are far away from the inversion sites. The atoms need to be moved by ∼50% of the lattice constants for at least four atoms (two $X$ and two $Y$) to preserve the inversion symmetry. Therefore, the crystal lattice structure in this class of compounds is far away from inversion symmetry.

Furthermore, the atoms at the $X$ and $Y$ sites are nearly in the ionic form with strong local charge and spin orbital coupling (SOC). Therefore, both giant spin-orbit splitting and large shift currents are expected. Very recently, a giant Dresselhaus spin-orbit splitting at the top of the valence bands was observed in one of these compounds, IrBiSe, via a good agreement between angle-resolved photoemission spectroscopy (ARPES) measurements and density functional theory (DFT) calculations. This implies the accuracy of the first principles in this class of compounds [35].

The shift current $J_{\rm shift}(\omega)$ is generated by an electrical field $\vec{E}(t) = \vec{E}(\omega)e^{i\omega t} + \vec{E}(-\omega)e^{-i\omega t}$ with photon energy $\hbar\omega$ via the second-order response $J^c_{\rm shift}(\omega) = \sigma^c_{ab}(\omega)E_a(\omega)E^*_b(\omega)$ [11,13,14,18]. The photoconductivity $\sigma^c_{ab}$ is calculated by the quadratic response theory in the clean limit [11,13,14,36],

$$\sigma^c_{ab} = \frac{|e|^3}{8\pi^3\omega^2}\,\mathrm{Re}\left(\sum_{E_\omega=\pm\hbar\omega}\sum_{l,m,n}\int_{BZ} d^3k(f_l - f_n)\Omega^{abc}_{l,m,n}(\omega)\right), \tag{1}$$

$$\Omega^{abc}_{l,m,n}(\omega) = \frac{\langle n|\hat{v}_a|l\rangle\langle l|\hat{v}_b|m\rangle\langle m|\hat{v}_c|n\rangle}{(E_n - E_m - i\delta)(E_n - E_l + E_\omega - i\delta)}, \tag{2}$$

where $|n\rangle$ is an eigenvector of the Hamiltonian with eigenvalue $E_n$ at point $\vec{k}$ and $\hat{v}_a = \frac{\hat{p}_a}{m_0}$ is the velocity operator. The details of deriving the formalism were discussed in Ref. [11,13,14,36] To calculate the second-order photoconductivity, we projected the *ab initio* DFT Bloch wave function into atomic-orbital-like Wannier functions [37] with diagonal position operator, as performed in the code of the full-potential local-orbital (FPLO) minimum basis [38,39]. To ensure the accuracy of the Wannier projection, we have included the outermost $d$, $s$, and $p$ orbitals for transition metals (such as the $5d$, $6s$, and $6p$ orbitals for Ir) and the outermost $s$ and $p$ orbitals for main-group elements. Based on the highly symmetric Wannier functions, we constructed an effective tight-binding model Hamiltonian and calculated the photoconductivity by following formula (1). A dense $k$ grid of $480 \times 480 \times 480$ was used for the integral.

## III. RESULTS AND DISCUSSION

Because all these compounds share the same symmetry operations and similar electronic band structures, we consider only two cases as examples for detailed analysis. One of them is RhBiS, with the largest shift current in this family of materials, and the other is IrBiSe, with already confirmed band structure by recent ARPES measurement [35]. The energy dispersions of RhBiS and IrBiSe are shown in Figs. 1(c) and 1(d), respectively. Both of them are semiconductors with band gaps around 0.5 eV. Because the tops of the occupied bands are dominated by the Bi-$6p$ orbital, SOC leads to a large spin splitting on the top of the valence bands, owing to the absence of an inversion center, which is fully consistent with recent ARPES measurements. In addition, these classes of compounds host interesting band structures of triple point fermions protected by the $c_3$ rotation symmetry and Weyl points with opposite chiralities at different Fermi levels because of the absence of mirror symmetry. These side

products of our work will be discussed in detail in future independent reports.

In these compounds, the indirect band gap with SOC is smaller compared to the case without SOC due to the spin split (see the dispersion in the Γ-*M* direction), and the size of the decrease depends on the strength of SOC. In addition, a direct result of the SOC spin splitting is the decrease in the density of states (DOS) near the top of the valence bands, from which we expect the decrease in the joint DOS and the size of the photoconductivity for frequencies close to the band gap.

Based on the second-order response theory, $J^c_{\text{shift}}(\omega) = \sigma^c_{ab}(\omega)E_a(\omega)E^*_b(\omega)$, the photoconductivity obtains a negative sign by inverting each of the indices. For the specified point group $T$, the three $c_2$ symmetries with respect to the $x$, $y$, or $z$ axes play the crucial role of deciding the shape of the photoconductivity tensor. For example, the rotation operation of $c_{2z}$ will change the sign of the tensor elements with even multiples of the $z$ index, and therefore force them to be zero. A similar rule also applies to $c_{2x}$ and $c_{2y}$. Further, because of the $D_2$ subgroup, the three indexes give the same photoconductivity, and there is only one independent tensor element for the photoconductivity tensor in the shape of

$$\underline{\sigma}^x = \begin{pmatrix} 0 & 0 & 0 \\ 0 & 0 & \sigma \\ 0 & \sigma & 0 \end{pmatrix}, \quad \underline{\sigma}^y = \begin{pmatrix} 0 & 0 & \sigma \\ 0 & 0 & 0 \\ \sigma & 0 & 0 \end{pmatrix},$$
$$\underline{\sigma}^z = \begin{pmatrix} 0 & \sigma & 0 \\ \sigma & 0 & 0 \\ 0 & 0 & 0 \end{pmatrix}. \tag{3}$$

Our calculated results are fully consistent with the symmetry analysis. Without considering SOC, RhBiS obtains the maximum value of $\sim -100\ \mu\text{A/V}^2$ with photon energy ~1.5 eV; see Fig. 2(a). SOC shifts the whole curve of the energy dependent photoconductivity to a lower frequencies by an amount ~0.3 eV. The peak is moved to a relatively small photon energy of ~1.4 eV, and the maximum value is reduced to $\sim 80\ \mu\text{A/V}^2$. Similar behavior can be also found in IrBiSe; see Fig. 2(b). Without including SOC, the photoconductivity presents two peak values that can reach $100\ \mu\text{A/V}^2$ with photon energies of ~2.1 and ~2.5 eV, respectively. After taking SOC into consideration, the photoconductivity reduces to only $\sim 50\ \mu\text{A/V}^2$. This decrease is larger than that in RhBiS, possibly due to stronger SOC. Hence, SOC plays a negative role for the shift current, as expected from band structure analysis.

The comparison of photoconductivity among the compounds reported in the previous literature and the semiconductors in this work is given in Fig. 2(c). Two typical cases are the ferroelectrics $BaTiO_3$ and $PbTiO_3$, in which the photoconductivities are $\sim 5\ \mu\text{A/V}^2$ for photoenergy in the visible range. So far, the largest photoconductivity in the visible spectrum range is $\sim 6\ \mu\text{A/V}^2$, observed in SbSI [41] in 2018. In the class of semiconductors of the present work, the photoconductivity can range from $\sim 20\ \mu\text{A/V}^2$ to $\sim 80\ \mu\text{A/V}^2$, comparable to the largest reported photoconductivity in the semiconductors.

Normally, the decrease of photoconductivity by SOC only works in simple band structures, where we assumed that the system contains a few bands only and that the subbands after the SOC spin split do not mix with each other. If the band structure is complicated and has strong hybridization, SOC might change the band orders and contribute positively to the shift current. SOC also complicates the hybridization of different bands for this class of compounds; see Figs. 1(c) and 1(d). As shown in Fig. 2(c), the photoconductivity decreases after the inclusion of SOC for most of the insulators in this class of compounds. The only two exceptions are IrSbTe and IrBiS, in which different effects from spin splitting compete and almost cancel each other.

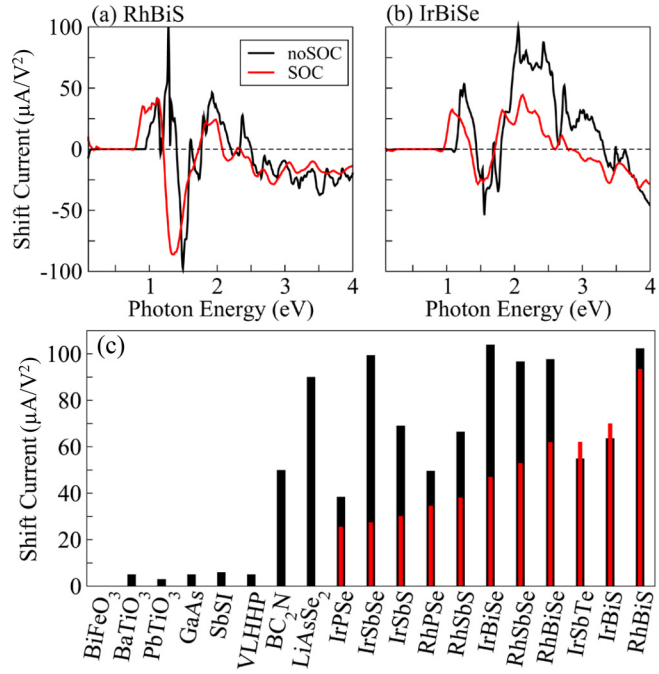


FIG. 2. Three-dimensional shift currents for the insulators in the class of compounds *MXY* considered here and other real materials reported previously. (a,b) Energy-dependent shift current for RhBiS and IrBiSe, respectively. (c) Comparison of the maximum values of shift currents with visible spectrum among the insulators obtained in this work and those reported in previous works. The calculated results without and with the inclusion of SOC are presented by black and red lines, respectively. VLHHP means vinylene-linked hybrid heterocyclic polymer. The data for the shift currents are from [24–29,40,41].

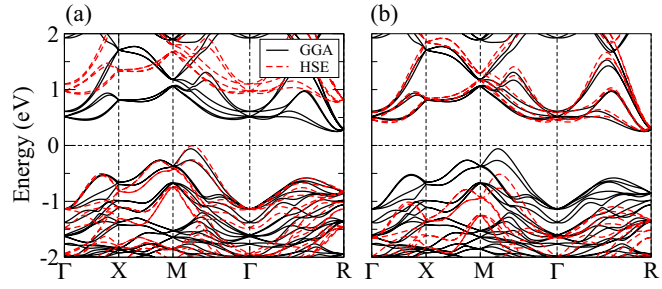


FIG. 3. Comparison of energy dispersions of RhBiS calculated from GGA and hybride functionals. (a) The comparison for the valence bands. (b) The comparison for the conduction bands. The calculations were performed using the Vienna Ab initio Simulation Package (VASP) [42,43]

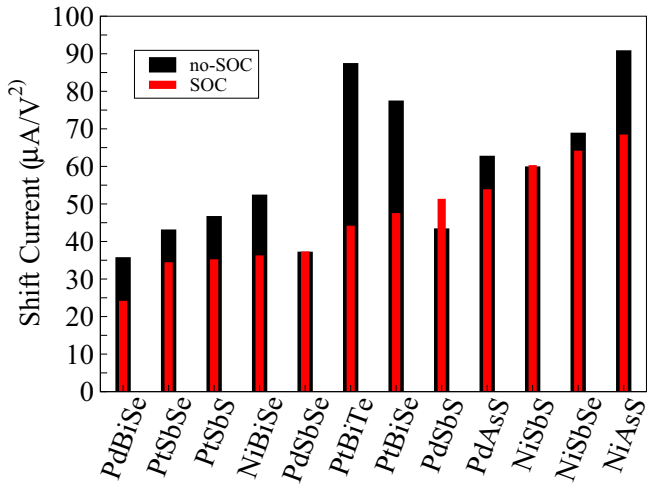


FIG. 4. Peak value of three-dimensional shift currents in the visible spectrum of metals studied in this work. The calculated results without and with the inclusion of SOC are presented by black and red lines, respectively.

Because the DFT calculations with generalized gradient approximations (GGAs) normally underestimate the band gap in insulators [39], we double checked the band structures by using a more accurate hybrid functional [44]. It is found that the only difference in the band structures from the two types of approximations is the band gap, and the shapes of the bands almost do not change for both valence and conduction bands near the band gap; see Fig. 3. Hence, we believe that the maximum values of the photoconductivity should also shift to higher frequencies, while keeping the magnitude almost unchanged. The comparison between the band structures from the hybrid functional and GGA calculations yields that the frequency shift is around 0.5 eV.

Very recently, considerable interest regarding BPVE was devoted to metallic systems, as the natural requirement of inversion symmetry breaking for BPVE can also lead to topological Weyl semimetals (WSMs) with monopoles of Berry curvature and linear energy dispersion [30,45–47]. The gapless electronic band structure with inversion symmetry broken provides the possibility to extend BPVE into the long wavelength range. Indeed, strong shift current can be also obtained in inversion-symmetry-broken metals. In this class of compounds, there are 12 metals with a transition metal atom sitting at $M$ = Ni, Pd, and Pt, where the photoconductivity can range from ∼30 to ∼60 $\mu A/V^2$ in the visible spectrum range, around one order magnitude larger than that reported for ferroelectrics. Similar to the insulators, SOC also plays a negative role most of the time; see Fig. 4.

## IV. SUMMARY

In summary, we theoretically predicted strong shift currents in chiral crystal materials. The three-dimensional photoconductivity can range from ∼20 to ∼80 $\mu A/V^2$, comparable to the largest reported photoconductivity in the insulators and semiconductors. Via electronic band structure analysis, we found that SOC plays a negative role in most cases for the shift current. This class of compounds provides a good platform to study the mechanism of the PBVE and its future applications. It illustrates that chiral crystals can host not only quantized CPGE but also a strong shift current, which is of great technological importance.

## ACKNOWLEDGMENTS

This work was financially supported by the ERC Advanced Grant No. 291472 "Idea Heusler" and ERC Advanced Grant No. 742068 "TOPMAT." This work was performed in part at the Center for Nanoscale Systems (CNS), a member of the National Nanotechnology Coordinated Infrastructure Network (NNCI), which is supported by the National Science Foundation under NSF Award No. 1541959. CNS is part of Harvard University. Some of our calculations were carried out on the Cobra cluster of MPCDF, Max Planck Society.

[1] J. L. Manes, Phys. Rev. B **85**, 155118 (2012).
[2] B. Bradlyn, J. Cano, Z. Wang, M. Vergniory, C. Felser, R. Cava, and B. A. Bernevig, Science **353**, aaf5037 (2016).
[3] N. B. M. Schröter, D. Pei, M. G. Vergniory, Y. Sun, K. Manne, F. d. Juan, J. A. Krieger, V. Süss, M. Schmidt, P. Dudin, B. Bradlyn, T. K. Kim, T. Schmitt, C. Cacho, C. Felser, V. N. Strocov, and Y. Chen, Nat. Phys. **15**, 759 (2019).
[4] P. Tang, Q. Zhou, and S.-C. Zhang, Phy. Rev. Lett. **119**, 206402 (2017).
[5] G. Chang, S.-Y. Xu, B. J. Wieder, D. S. Sanchez, S.-M. Huang, I. Belopolski, T.-R. Chang, S. Zhang, A. Bansil, H. Lin *et al.*, Phy. Rev. Lett. **119**, 206401 (2017).
[6] G. Chang, B. J. Wieder, F. Schindler, D. S. Sanchez, I. Belopolski, S.-M. Huang, B. Singh, D. Wu, T.-R. Chang, T. Neupert *et al.*, Nat. Mater. **17**, 978 (2018).
[7] F. de Juan, A. G. Grushin, T. Morimoto, and J. E. Moore, Nat. Commun. **8**, 15995 (2017).
[8] F. Flicker, F. de Juan, B. Bradlyn, T. Morimoto, M. G. Vergniory, and A. G. Grushin, Phys. Rev. B **98**, 155145 (2018).
[9] D. Rees, K. Manna, B. Lu, T. Morimoto, H. Borrmann, C. Felser, J. E. Moore, D. H. Torchinsky, and J. Orenstein, arXiv:1902.03230.
[10] W. Shockley and H. J. Queisser, J. Appl. Phys. **32**, 510 (1961).
[11] W. Kraut and R. von Baltz, Phys. Rev. B **19**, 1548 (1979).
[12] V. Belinicher and B. Sturman, Phys. Usp. **23**, 199 (1980).
[13] N. Kristoffel and A. Gulbis, Z. Phys. B: Condens. Matter **39**, 143 (1980).
[14] R. von Baltz and W. Kraut, Phys. Rev. B **23**, 5590 (1981).
[15] N. Kristoffel, R. Von Baltz, and D. Hornung, Z. Phys. B: Condens. Matter **17**, 293 (1982).
[16] H. Presting and R. Von Baltz, Phys. Status Solidi B **112**, 559 (1982).
[17] C. Aversa and J. E. Sipe, Phys. Rev. B **52**, 14636 (1995).
[18] J. E. Sipe and A. I. Shkrebtii, Phys. Rev. B **61**, 5337 (2000).

[19] K. Yao, B. K. Gan, M. Chen, and S. Shannigrahi, Appl. Phys. Lett. **87**, 212906 (2005).
[20] Q. Ma, S.-Y. Xu, C.-K. Chan, C.-L. Zhang, G. Chang, Y. Lin, W. Xie, T. Palacios, H. Lin, S. Jia *et al.*, Nat. Phys. **13**, 842 (2017).
[21] S.-Y. Xu, Q. Ma, H. Shen, V. Fatemi, S. Wu, T.-R. Chang, G. Chang, A. M. M. Valdivia, C.-K. Chan, Q. D. Gibson *et al.*, Nat. Phys. **14**, 900 (2018).
[22] T. Morimoto, M. Nakamura, M. Kawasaki, and N. Nagaosa, Phys. Rev. Lett. **121**, 267401 (2018).
[23] W. Ji, K. Yao, and Y. C. Liang, Adv. Mater. **22**, 1763 (2010).
[24] S. M. Young and A. M. Rappe, Phy. Rev. Lett. **109**, 116601 (2012).
[25] F. Zheng, H. Takenaka, F. Wang, N. Z. Koocher, and A. M. Rappe, J. Phys. Chem. Lett. **6**, 31 (2014).
[26] J. A. Brehm, S. M. Young, F. Zheng, and A. M. Rappe, J. Chem. Phys. **141**, 204704 (2014).
[27] A. Von Hippel, Rev. Mod. Phys. **22**, 221 (1950).
[28] J. Shieh, J. Yeh, Y. Shu, and J. Yen, Mater. Sci. Eng. B **161**, 50 (2009).
[29] S. Liu, F. Zheng, and A. M. Rappe, J. Phys. Chem. C **121**, 6500 (2017).
[30] A. M. Cook, B. M. Fregoso, F. De Juan, S. Coh, and J. E. Moore, Nat. Commun. **8**, 14176 (2017).
[31] T. Rangel, B. M. Fregoso, B. S. Mendoza, T. Morimoto, J. E. Moore, and J. B. Neaton, Phy. Rev. Lett. **119**, 067402 (2017).
[32] J. A. Brehm, J. Mater. Chem. C **6**, 1470 (2018).
[33] J. Ibañez-Azpiroz, I. Souza, and F. de Juan, arXiv:1906.07627.
[34] F. Hulliger, Nature (London) **198**, 382 (1963).
[35] Z. Liu, S. Thirupathaiah, A. Yaresko, S. Kushwaha, Q. Gibson, R. Cava, and S. Borisenko, arXiv:1705.07431.
[36] Y. Zhang, H. Ishizuka, J. van den Brink, C. Felser, B. Yan, and N. Nagaosa, Phys. Rev. B **97**, 241118(R) (2018).
[37] J. R. Yates, X. Wang, D. Vanderbilt, and I. Souza, Phys. Rev. B **75**, 195121 (2007).
[38] K. Koepernik and H. Eschrig, Phys. Rev. B **59**, 1743 (1999).
[39] J. P. Perdew, K. Burke, and M. Ernzerhof, Phys. Rev. Lett. **77**, 3865 (1996).
[40] D. Côté, N. Laman, and H. Van Driel, Appl. Phys. Lett. **80**, 905 (2002).
[41] M. Sotome, M. Nakamura, J. Fujioka, M. Ogino, Y. Kaneko, T. Morimoto, Y. Zhang, M. Kawasaki, N. Nagaosa, Y. Tokura *et al.*, Proc. Natl. Acad. Sci. USA **116**, 1929 (2019).
[42] G. Kresse and J. Hafner, Phys. Rev. B **48**, 13115 (1993).
[43] G. Kresse and J. Furthmüller, Comput. Mater. Sci. **6**, 15 (1996).
[44] J. Heyd, G. E. Scuseria, and M. Ernzerhof, J. Chem. Phys. **118**, 8207 (2003).
[45] G. B. Osterhoudt, L. K. Diebel, M. J. Gray, X. Yang, J. Stanco, X. Huang, B. Shen, N. Ni, P. J. W. Moll, Y. Ran, and K. S. Burch, Nat. Mater. **18**, 471 (2019).
[46] M.-M. Yang, D. J. Kim, and M. Alexe, Science **360**, 904 (2018).
[47] T. Morimoto and N. Nagaosa, Sci. Adv. **2**, e1501524 (2016).